

# Heat capacities and thermodynamic properties of a novel mixed-ligands MOFs

Li-Fang Song · Chun-Hong Jiang · Jian Zhang · Li-Xian Sun ·  
Fen Xu · Wan-Sheng You · Yi Zhao · Zhi-Heng Zhang · Mei-Han Wang ·  
Yutake Sawada · Zhong Cao · Ju-Lan Zeng

Received: 31 March 2009 / Accepted: 5 June 2009 / Published online: 9 July 2009  
© Akadémiai Kiadó, Budapest, Hungary 2009

**Abstract** A novel metal-organic frameworks  $[\text{Cu}_2(\text{OH})(2,2'\text{-bpy})_2(\text{BTC}) \cdot 2\text{H}_2\text{O}]_n$  (CuMOF, BTC = benzene-1,3,5-tricarboxylic acid, 2,2'-bpy = 2,2'-bipyridine) has been synthesized hydrothermally and characterized by single crystal XRD, FT-IR spectra. The low-temperature molar heat capacities were measured by temperature modulated differential scanning calorimetry (TMDSC) for the first time. The thermodynamic parameters such as entropy and enthalpy relative to reference temperature 298.15 K were derived based on the above molar heat capacity data. Moreover, the thermal stability and the decomposition mechanism of CuMOF were investigated by

TG-MS (thermogravimetry-mass spectrometer). A four-stage mass loss was observed in the TG curve. MS curve indicated that the gas products for oxidative degradation of CuMOF were  $\text{H}_2\text{O}$ ,  $\text{CO}_2$ , NO and  $\text{NO}_2$ .

**Keywords** Copper · Metal-organic frameworks · Molar heat capacity · Temperature modulated differential scanning calorimetry · Thermogravimetry

## Introduction

In the past decade, many metal-organic frameworks have been synthesized, providing a variety of properties ranging from gas storage [1], ion exchange [2], catalysis [3], chemical sensor [4], and separation [5] by their frameworks. This class of materials can be easily obtained through self-assembly of a potentially multifunctional ligand with a metal ion that has more than one vacant or labile site. The bipyridine and polycarboxylate are the most common polyfunctional organic linkers to form mixed-ligands frameworks [6]. The bipyridine ligands can combine different aromatic carboxylate co-ligands to assemble into diverse polymeric frameworks consisting of one-, two- or three-dimensional structures.

Molar heat capacities of the materials at different temperatures are basic data in chemistry and engineering, from which many other thermodynamic properties such as enthalpy and entropy can be calculated. These parameters are important for both theoretical and practical purposes. Heat capacities determinations of various compounds have attracted many researchers' attention [7, 8].

It is generally accepted that heat capacity is one of the most fundamental thermodynamic properties of substances and that it is closely related to other physical and chemical

---

L.-F. Song · C.-H. Jiang · J. Zhang · L.-X. Sun (✉)  
Materials and Thermochemistry Laboratory, Dalian Institute of Chemical Physics, Chinese Academy of Sciences, 457 Zhongshan Road, 116023 Dalian, People's Republic of China  
e-mail: lxsun@dicp.ac.cn

L.-F. Song · C.-H. Jiang  
Graduate School of the Chinese Academy of Sciences,  
100049 Beijing, People's Republic of China

F. Xu · W.-S. You · Y. Zhao  
Faculty of Chemistry and Chemical Engineering, Liaoning Normal University, 116029 Dalian, People's Republic of China

Z.-H. Zhang  
Applied Chemistry Institute of R & D Center of PetroChina Pipeline Company, 51 Jinguang Road, 065000 Langfang, Hebei, People's Republic of China

M.-H. Wang · Y. Sawada  
Department of Nanochemistry, Faculty of Engineering, Tokyo Polytechnic University, Atsugi, Kanagawa 2430297, Japan

Z. Cao · J.-L. Zeng  
School of Chemistry & Biological Engineering, Changsha University of Science & Technology, 410076 Changsha, China

properties. Temperature modulated differential scanning calorimetry (TMDSC) is one of easier and more accurate methods for determining heat capacity. In 1992, TMDSC was initially proposed by Reading and et al. [9], who applied a small sinusoidal modulation of temperature superimposed onto a linear underlying heating rate as an extension of the conventional DSC. The structure and principle of the calorimeter have been described in detail by the literatures [10–12]. Recently, this method has been greatly developed for directly determining heat capacities for various materials isothermally and non-isothermally [7, 8, 13–15].

In the present article, we reported one novel mixed-ligands metal-organic frameworks. The low-temperature molar heat capacities of the compound were measured by TMDSC and the thermodynamic parameters such as entropy and enthalpy were also calculated. The accuracy of TMDSC was established by comparing the measured heat capacities of standard sapphire ( $\alpha$ -Al<sub>2</sub>O<sub>3</sub>) with previously reported values (NIST and NBS) [16, 17]. The thermal decomposition characteristics of this compound were investigated by TG-MS.

## Experimental

All materials were commercially available and were of analytical grade unless stated elsewhere.

### Sample preparation

[Cu<sub>2</sub>(OH)(2,2'-bpy)<sub>2</sub>(BTC) · 2H<sub>2</sub>O]<sub>n</sub> was prepared by hydrothermal reaction. A mixture of Cu(CH<sub>3</sub>COO)<sub>2</sub> · H<sub>2</sub>O (0.199 g, 1 mmol), H<sub>3</sub>BTC (0.141 g, 0.67 mmol), 2,2'-bpy (0.156 g, 1 mmol), NaOH (0.080 g, 2 mmol) and H<sub>2</sub>O (15 mL) was sealed in a 40 mL Teflon-lined stainless steel autoclave and heated at 120 °C for 24 h, then cooled to room temperature naturally. Dark blue block crystals suitable to single crystal X-ray diffraction analysis were obtained in ca. 52% yield based on Cu (II). After filtration, the product was washed with distilled water and then dried at 50 °C under vacuum overnight.

### Characterization

The crystal data were collected at 293 K using a SMART APEX II-CCD single crystal XRD (graphite monochromated MoK $\alpha$  radiation,  $\lambda = 0.71073$  Å). A multi-scan absorption correction was applied using the SADABS program. The structures were solved by direct methods and refined by full-matrix least-squares method implemented in SHELXTL-97 [18]. All the non-hydrogen atoms were refined anisotropically. Hydrogen atoms were added

theoretically. FT-IR spectra were recorded on a Nicolet 380 FT-IR spectrometer using KBr pellet in the wavelength range of 4000–400 cm<sup>-1</sup>.

Crystal data for the CuMOF were as follows: triclinic system, P-1 (no. 2),  $a = 8.7523(15)$ ,  $b = 9.9715(17)$ ,  $c = 17.610(3)$ ,  $\alpha = 92.857(2)$ ,  $\beta = 104.123(2)$ ,  $\gamma = 107.665(2)$ . The molar mass of CuMOF is 699.62. Before thermal experiments, the sample was heated at 323 K in vacuum for 6 h.

The presence of coordinated H<sub>2</sub>O molecules caused the appearance of strong and broad  $\nu(\text{O-H})$  stretching bands centered at 3715–2778 cm<sup>-1</sup>. Characteristic vibrations of aromatic nucleus [ $\nu(\text{C-C})$ ,  $\nu(\text{C-N})$ ] are near 1610 and 1574 cm<sup>-1</sup>, while  $\nu(\text{C-H})$  deformation vibrations are about 771 cm<sup>-1</sup> and 720 cm<sup>-1</sup> (phen). The most salient feature in the IR spectra was the existence of two very strong bands at 1,560 and 1,360 cm<sup>-1</sup>, attributed to the  $\nu_{\text{as}}(\text{COO})$  and  $\nu_{\text{s}}(\text{COO})$  stretching vibrations of the BTC ligand.

### Heat capacity measurement

Heat capacity measurements were performed on DSC Q1000 (T-zero DSC-technology, TA Instruments Inc., USA). A mechanical cooling system was used for the experimental measurement and dry nitrogen gas with high purity (99.999%) was used as purge gas (50 mL min<sup>-1</sup>) through the DSC cell. The temperature scale of the instrument was initially calibrated in the standard DSC mode, using the extrapolated onset temperatures of the melting of indium (429.75 K) at a heating rate of 10 K min<sup>-1</sup>. The energy scale was calibrated with the heat of fusion of indium (28.45 J g<sup>-1</sup>). The heat capacity calibration was made by running a standard sapphire ( $\alpha$ -Al<sub>2</sub>O<sub>3</sub>) at the experimental temperature. The calibration method and the experiment were performed at the same conditions as follows: 1) sampling interval: 1.00 s/pt; 2) zero heat flow at 253.15 K; 3) equilibrate at 133.15 K; 4) modulate temperature amplitude of  $\pm 0.5$  K with period of 100 s; 5) isothermal for 5.00 min; 6) temperature ramp at 5 K min<sup>-1</sup> to 413 K. The constants of heat capacity for the TMDSC:  $K_{\text{total}} = 1.024$ ;  $K_{\text{reversible}} = 1.019$ .

The masses of the reference and sample pans with lids were measured to within  $30 \pm 0.05$  mg. Samples were crimped in non-hermetic aluminum pans with lids. Sample mass was weighed on a METTLER TOLEDO electrobalance (AB135-S, Classic) with an accuracy of ( $\pm 0.01$  mg).

### Thermal analysis

Thermogravimetric analysis (TG) was carried out on Cahn Thermax 500 from 300–873 K. The heating rate was 10 K min<sup>-1</sup> and the flow rate of air was 100 mL min<sup>-1</sup>. The sample mass of the CuMOF was 24.67 mg. The TG

equipment was calibrated by the  $\text{CaC}_2\text{O}_4 \cdot \text{H}_2\text{O}$  (99.9%). Mass spectra (MS) were performed on a Multicomponent Online Gas Analyzer GAM 200.

## Results and discussion

Heat capacity of standard sapphire ( $\alpha\text{-Al}_2\text{O}_3$ )

Heat capacity measurements were repeated three times unless stated elsewhere. The emphasis of this work is to assess the reproducibility and ensure accuracy of the measured data using TMDSC (Q1000). For sapphire measurement, the data of three reduplicate experiments and the experimental standard deviation for standard sapphire were given in our previous work [8]. The experimental standard deviation is during  $\pm 0.20$ , and the result shows that the testing system of TMDSC is steady. Relative deviations have been calculated by the following equation:

$$\text{RD}(\%) = 100 [C_{p,m}(\text{exp}) - C_{p,m}(\text{ref})] / C_{p,m}(\text{ref}) \quad (1)$$

where  $C_{p,m}(\text{exp})$  is the experimental heat capacities and  $C_{p,m}(\text{ref})$  is the referenced heat capacities. The results show that the relative deviation of our calibration data from the recommended value [16] over the whole temperature range was within  $\pm 1.5\%$ .

Heat capacity of CuMOF

The data of four reduplicate experiments and the experimental standard deviation for CuMOF are given in Table 1. The experimental standard deviations below 0.04 are obtained and show reasonably good reproducibility in the temperature range from 190–320 K. The experimental molar heat capacities curve of CuMOF versus temperature is shown in Fig. 1. The experimental and simulated molar heat capacities data are listed in Table 2.

The molar heat capacities of the sample are fitted to the following polynomial equation of heat capacities ( $C_{p,m}$ ) with reduced temperature ( $X$ ) by means of the least square fitting:

From  $T = (190\text{--}320)$  K,

$$C_{p,m} [\text{J mol}^{-1} \text{K}^{-1}] = 646.8 + 150.6X + 20.05X^2 + 69.66X^3 + 94.50X^4 + 36.54X^5 \quad (2)$$

where  $X = (T - 255)/65$ , and  $T$  is the experimental temperature, 255 is obtained from polynomial  $(T_{\text{max}} + T_{\text{min}})/2$ , 65 is obtained from polynomial  $(T_{\text{max}} - T_{\text{min}})/2$ ,  $T_{\text{max}}$  is the upper limit (320 K) of the above temperature region,  $T_{\text{min}}$  is the lower limit (190 K) of the above temperature region. The correlation coefficient of the fitting,  $R^2 = 0.99992$ . The relative deviations of all the experimental points from the fitting heat-capacity values are

**Table 1** The data of four reduplicate experiments for CuMOF

$T/\text{K}$	$C_{p,m}(\text{exp})/\text{J K}^{-1} \text{g}^{-1}$					Standard deviation
	$a$	$b$	$c$	$d$	Average	
190	0.7520	0.7265	0.6986	0.7143	0.7229	0.023
195	0.7639	0.7387	0.7103	0.7265	0.7349	0.023
200	0.7769	0.7514	0.7216	0.7391	0.7473	0.023
205	0.7915	0.7669	0.7353	0.7542	0.7620	0.024
210	0.8077	0.7831	0.7516	0.7710	0.7784	0.023
215	0.8234	0.7992	0.7677	0.7876	0.7945	0.023
220	0.8400	0.8156	0.7840	0.8040	0.8109	0.023
225	0.8561	0.8320	0.8001	0.8337	0.8305	0.023
230	0.8720	0.8484	0.8165	0.8410	0.8445	0.023
235	0.8878	0.8645	0.8320	0.8557	0.8600	0.023
240	0.9039	0.8801	0.8473	0.8711	0.8756	0.023
245	0.9204	0.8958	0.8629	0.8861	0.8913	0.024
250	0.9356	0.9106	0.8781	0.9014	0.9064	0.024
255	0.9507	0.9257	0.8918	0.9156	0.9210	0.024
260	0.9701	0.9445	0.9099	0.9338	0.9396	0.025
265	0.9884	0.9625	0.9275	0.9516	0.9575	0.025
270	1.0090	0.9813	0.9467	0.9714	0.9771	0.026
275	1.0360	1.0040	0.9685	0.9928	1.0003	0.028
280	1.0590	1.0250	0.9932	1.0160	1.0233	0.027
285	1.0840	1.0490	1.0200	1.0440	1.0493	0.026
290	1.1150	1.0760	1.0520	1.0740	1.0793	0.026
295	1.1520	1.1080	1.0890	1.1080	1.1143	0.027
300	1.1970	1.1470	1.1370	1.1520	1.1583	0.027
305	1.2510	1.1940	1.1980	1.2050	1.2120	0.026
310	1.3190	1.2520	1.2760	1.2690	1.2790	0.029
315	1.3970	1.3210	1.3720	1.3440	1.3585	0.033
320	1.4900	1.4070	1.4960	1.4340	1.4568	0.043

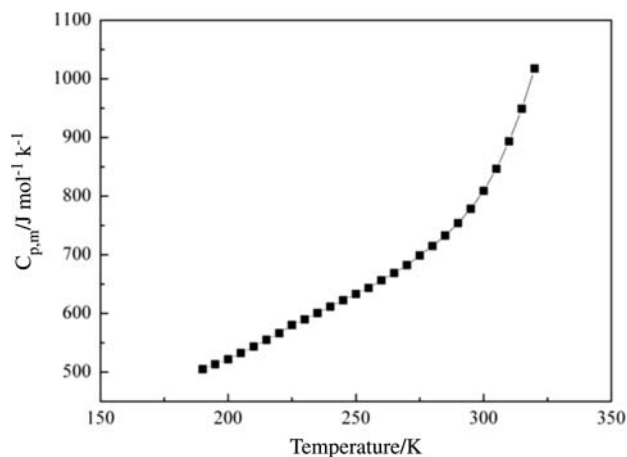


**Fig. 1** Molar heat capacities ( $C_{p,m}$ ) of CuMOF as a function of temperature

within  $\pm 0.48\%$  in Table 2. Based on Eq. 2, the heat capacity of the sample at 298.15 K was calculated to be  $799.1 \text{ J mol}^{-1} \text{K}^{-1}$ .

**Table 2** The experimental and simulated molar heat capacities of CuMOF

<i>T</i> /K	$C_{p,m}$ (exp)/J K <sup>-1</sup> mol <sup>-1</sup>	$C_{p,m}$ (fit)/J K <sup>-1</sup> mol <sup>-1</sup>	RD/%	<i>T</i> /K	$C_{p,m}$ (exp)/J K <sup>-1</sup> mol <sup>-1</sup>	$C_{p,m}$ (fit)/J K <sup>-1</sup> mol <sup>-1</sup>	RD/%
190	505.7	504.6	-0.23	260	657.3	658.5	0.18
195	514.1	514.2	0.016	265	669.9	670.8	0.13
200	522.8	524.1	0.25	270	683.6	683.8	0.025
205	533.1	534.4	0.24	275	699.8	698.0	-0.26
210	544.5	544.9	0.070	280	715.9	714.0	-0.26
215	555.8	555.8	0.0038	285	734.1	732.5	-0.22
220	567.3	566.9	-0.068	290	755.1	754.2	-0.12
225	581.0	578.2	-0.48	295	779.6	780.1	0.068
230	590.8	589.6	-0.20	300	810.3	811.3	0.12
235	601.7	601.1	-0.099	305	847.9	849.1	0.14
240	612.6	612.5	-0.014	310	894.8	895.1	0.030
245	623.6	623.9	0.053	315	950.4	950.8	0.037
250	634.2	635.3	0.18	320	1019	1018	-0.10
255	644.3	646.8	0.39				

From Fig. 1, it can be seen that the heat capacity of the sample increases with increasing temperature continuously in the temperature range from 190–320 K. No phase transition or thermal anomaly was observed in the experimental temperature range. This indicates that the sample is stable in this temperature region.

#### Thermodynamic functions of CuMOF

Enthalpy and entropy of substances are basic thermodynamic functions. In terms of the polynomials of molar heat capacity and the thermodynamic relationship, the [ $H_T - H_{298.15}$ ] and [ $S_T - S_{298.15}$ ] of CuMOF are calculated with an interval of 5 K relative to the temperature of 298.15 K. The thermodynamic relationships are as follows:

$$H_T - H_{298.15} = \int_{298.15}^T C_{p,m} dT \quad (3)$$

$$S_T - S_{298.15} = \int_{298.15}^T (C_{p,m}/T) dT \quad (4)$$

The calculated thermodynamic functions [ $H_T - H_{298.15}$ ] and [ $S_T - S_{298.15}$ ] are shown in Table 3.

#### Thermal stabilities and decomposition of CuMOF

TG curve (Fig. 2) of CuMOF shows that the four-stage mass loss occurs in the temperature range of 300–873 K. The first mass loss starts at about 340 K and is about 4.77% (calculated 5.15%), it is due to the dehydration from

**Table 3** Calculated thermodynamic function data of CuMOF

<i>T</i> /K	$H_T - H_{298.15}$ /kJ mol <sup>-1</sup>	$S_T - S_{298.15}$ /J K <sup>-1</sup> mol <sup>-1</sup>	<i>T</i> /K	$H_T - H_{298.15}$ /kJ mol <sup>-1</sup>	$S_T - S_{298.15}$ /J K <sup>-1</sup> mol <sup>-1</sup>
190	-67.89	-278.3	260	-27.35	-97.97
195	-65.35	-265.1	265	-24.02	-85.33
200	-62.75	-252.0	270	-20.64	-72.68
205	-60.10	-239.0	275	-17.18	-60.00
210	-57.41	-226.0	280	-13.65	-47.27
215	-54.65	-213.0	285	-10.04	-34.45
220	-51.85	-200.1	290	-6.32	-21.51
225	-48.98	-187.2	295	-2.49	-8.386
230	-46.06	-174.3	298.15	0	0
235	-43.09	-161.5	300	1.49	4.985
240	-40.05	-148.7	305	5.63	18.69
245	-36.96	-136.0	310	9.99	32.84
250	-33.82	-123.3	315	14.60	47.56
255	-30.61	-110.6	320	19.52	63.05

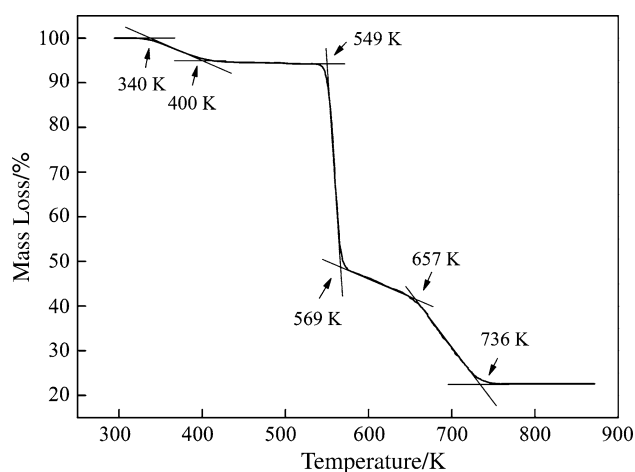


**Fig. 2** TG curve of CuMOF

$\text{Cu}_2(\text{OH})(2,2'\text{-bpy})_2(\text{BTC}) \cdot 2\text{H}_2\text{O}$  to  $\text{Cu}_2(\text{OH})(2,2'\text{-bpy})_2(\text{BTC})$ , which is confirmed in the MS curve ( $m/z = 18$ ) (Fig. 3a). Further decomposition in the region of 400–736 K is divided into three steps in a continuous way according to the degradation of the BTC and 2,2'-bpy ligands, so that the steps are not so clearly. The MS curve shows that the gas degradation products between 400 and 569 K are mainly  $\text{H}_2\text{O}$  ( $m/z = 18$ ),  $\text{CO}_2$  ( $m/z = 44$ ) (Fig. 3a) and little  $\text{NO}_2$  ( $m/z = 30, 46$ ) (Fig. 3b). The gas products of the temperature range of 569 to 631 K are mainly  $\text{H}_2\text{O}$  ( $m/z = 18$ ),  $\text{CO}_2$  ( $m/z = 44$ ) and  $\text{NO}$  ( $m/z = 30$ ) (Fig. 3b). The last decomposition stage is in the region of 657 to 736 K, the gas oxidation products are  $\text{H}_2\text{O}$  ( $m/z = 18$ ),  $\text{CO}_2$  ( $m/z = 44$ ),  $\text{NO}$  ( $m/z = 30$ ) and little  $\text{NO}_2$  ( $m/z = 30, 46$ ). The overall mass loss of the sample is about 77.82% in accord with the calculated percentage (77.26%), which indicates that the sample was probably decomposed to the  $\text{CuO}$ .

## Conclusions

In this work, one novel mixed-ligands metal-organic frameworks has been synthesized and characterized by single crystal X-ray diffraction and FT-IR spectra. The molar heat capacities of the compound were measured using TMDSC for the first time. The heat capacity of the sample at 298.15 K was calculated to be  $799.1 \text{ J mol}^{-1} \text{ K}^{-1}$ . The thermodynamic function data relative to the reference temperature (298.15 K) were calculated based on the heat capacities measurements. Moreover, the thermal stability of the compound was further investigated by TG-MS.

**Acknowledgements** The authors gratefully acknowledge the National Nature Science Foundation of China under Grant No.

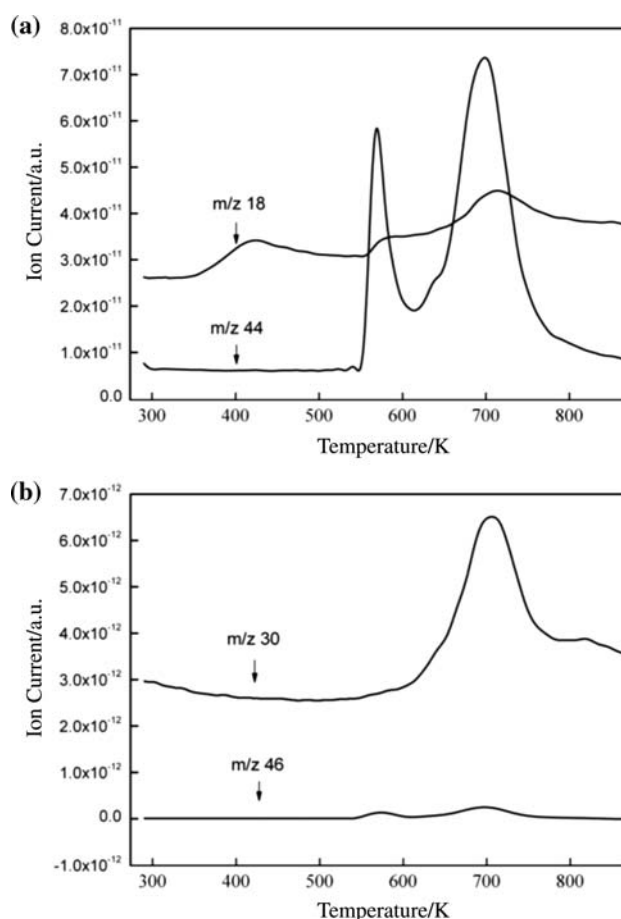


**Fig. 3** MS curve of CuMOF: **a**  $m/z = 18, 44$ , **b**  $m/z = 30, 46$

50671098, U0734005 and the Chinese National High Tech. “863” program No. 2007AA05Z102 and 2007AA05Z115 for financial support to this work.

## References

1. Yang W, Lin X, Jia J, Blake AJ, Wilson C, Hubberstey P, et al. A biporous coordination framework with high  $\text{H}_2$  storage density. *Chem Commun.* 2008;359–61.
2. Lu WG, Su CY, Lu TB, Jiang L, Chen JM. Two stable 3D metal-organic frameworks constructed by nanoscale cages via sharing the single-layer walls. *J Am Chem Soc.* 2006;128:34–5.
3. Xamena FXLI, Abad A, Corma A, Garcia H. MOFs as catalysts: activity, reusability and shape-selectivity of a Pd-containing MOF. *J Catal.* 2007;250:294–8.
4. Liu YY, Zhang J, Xu F, Sun LX, Zhang T, You WS, et al. Lithium-based 3D coordination polymer with hydrophilic structure for sensing of solvent molecules. *Cryst Growth Des.* 2008;8:3127–9.
5. Bae YS, Mulfort KL, Frost H, Ryan P, Punnathanam S, Broadbelt LJ, et al. Separation of  $\text{CO}_2$  from  $\text{CH}_4$  using mixed-ligand metal-organic frameworks. *Langmuir.* 2008;24:8592–8.
6. Park HJ, Suh MP. Mixed-ligand metal-organic frameworks with large pores: gas sorption properties and single-crystal-to-single-crystal transformation on guest exchange. *Chem Eur J.* 2008;14:8812–21.

7. Xue B, Li XF, Wang JY, Yu SJ, Tan ZC, Sun LX. Heat capacities and thermodynamic properties of trans-(R)-3-(2,2-dichloroethenyl)-2,2-dimethylcyclopropanecarboxylic acid. *J Therm Anal Calorim.* 2008;94:529-34
8. Qiu SJ, Chu HL, Zhang J, Qi YN, Sun LX, Xu F. Heat capacities and thermodynamic properties of CoPc and CoTMPP. *J Therm Anal Calorim.* 2008;91:841-8.
9. Reading M, Elliot D, Hill V. In: *Proceedings of the 21st North American Thermal Analysis Society Conference*; 1992. p. 145-50.
10. Wunderlich B, Jin Y, Boller A. Mathematical-description of differential scanning calorimetry based on periodic temperature modulation. *Thermochim Acta.* 1994;238:277-93.
11. Danley RL. New modulated DSC measurement technique. *Thermochim Acta.* 2003;402:91-8.
12. Wunderlich B. The contributions of MDSC to the understanding of the thermodynamics of polymers. *J Therm Anal Calorim.* 2006;85:179-87.
13. Divi S, Chellappa R, Chandra D. Heat capacity measurement of organic thermal energy storage materials. *J Chem Thermodyn.* 2006;38:1312-26.
14. Chau J, Garlicka I, Wolf C, Teh J. Modulated DSC as a tool for polyethylene structure characterization. *J Therm Anal Calorim.* 2007;90:713-9.
15. Qi YN, Xu F, Ma HJ, Sun LX, Zhang J, Jiang T. Thermal stability and glass transition behavior of PANI/gamma-Al<sub>2</sub>O<sub>3</sub> composites. *J Therm Anal Calorim.* 2008;91:219-23.
16. Archer DG. Thermodynamic properties of synthetic sapphire ( $\alpha$ -Al<sub>2</sub>O<sub>3</sub>), standard reference material 720 and the effect of temperature-scale differences on thermodynamic properties. *J Phys Chem Ref Data.* 1993;22:1441-53.
17. Ginnings DC, Furukawa GT. Heat capacity standards for the range 14°K to 1200°K. *J Am Chem Soc.* 1953;75:522-7.
18. Sheldrick GM. SHELX97, Program for crystal structure refinement. Germany: Göttingen University; 1997.